LASERS

PACS numbers: 42.55.Lt; 42.60.Lh
DOI: 10.1070/QE2000v030n10ABEH001824

Pulsed laser operating on the first overtone of the CO molecule in the 2.5 – 4.2-μm range. II. Frequency-selective lasing

N G Basov, A A Ionin, A A Kotkov, A K Kurnosov, J E McCord, A P Napartovich, L V Seleznev, N G Turkin, G D Hager

Abstract. Lasing properties of a pulsed electroionisation CO laser operating on the first overtone of the CO molecule in the frequency-selective regime were studied experimentally and theoretically. Lasing was observed on a large number of separate vibrational-rotational transitions $v + 2 \rightarrow v$ from $13 \rightarrow 11$ to $38 \rightarrow 36$ (more than 400 spectral lines) in the spectral range from 2.7 to 4.2 μm. The specific output energy of the overtone CO laser reached ~ 3.0 J l^{-1} amagat^{-1}, and the electrooptical conversion was ~ 0.6 %. The formation of emission spectra from high vibrational levels in the overtone CO laser observed for the first time is discussed. The comparison of experimental and theoretical data showed the necessity of including the multiquantum exchange on high vibrational levels into the kinetic model of the active medium of the CO laser.

1. Introduction

This work is a continuation of our studies reported in Ref. [1], where we experimentally and theoretically studied lasing properties of a pulsed electroionisation CO laser operating on the first overtone of the CO molecule in the multifrequency regime. The multifrequency overtone CO laser was shown to be an efficient source of coherent emission in the 2.5 – 4.1-μm range. The experimental laser efficiency exceeded 10 %, and the theoretical analysis showed the feasibility of obtaining efficiency as high as 20 %. The overtone laser emission on separate vibrational-rotational transitions has been earlier observed in a cw low-pressure CO laser [2 – 4] in the 2.62 – 4.07-μm range.

The aim of this work was to perform an experimental and theoretical study of spectral, energy, and temporal characteristics of emission of a pulsed CO laser operating in the frequency-selective regime on overtone vibrational-rotational transitions of the CO molecule. We compare experimental and theoretical data and discuss the emission from high vibrational levels, which we observed for the first time in the overtone CO laser.

N G Basov, A A Ionin, A A Kotkov, L V Seleznev P N Lebedev Physics Institute, Russian Academy of Sciences, Leninskii prosp. 53, 117924 Moscow, Russia; e-mail: aion@sci.lebedev.ru
A K Kurnosov, A P Napartovich, N G Turkin Troitsk Institute for Innovation and Thermonuclear Research, 142092 Troitsk, Moscow oblast, Russia; e-mail: apn@triniti.ru
J E McCord, G D Hager AFRL, Albuquerque, New Mexico, USA

Received 29 February 2000
Kvantovaya Elektronika **30** (10) 859 – 866 (2000)
Translated by A N Kirkin

2. Experimental

The output characteristics of the overtone CO laser operating in the frequency-selective regime were experimentally studied on a cryogenic (~ 100 K) electroionisation laser setup. The pump pulses were ~ 25 μs long, and a laser mixture had a density of 0.12 amagat. The experimental technique used for the measurement of energy deposition parameters and characteristics of laser radiation is described in Ref. [1].

A frequency-selective laser cavity was 3.0 m long. It was formed by a concave mirror (the radius of curvature was ~ 10 m), a copper mirror mounted on a laser chamber, and a diffraction grating (DG) operating in the autocollimation scheme, with laser emission outcoupled into the zero diffraction order. The DG was positioned on the cavity axis at a distance of ~ 0.4 m from the output window of the laser chamber, which represented a plane-parallel CaF_2 plate oriented at the Brewster angle to the optical axis of the cavity. Laser emission was linearly polarised in the plane of incidence on the DG, which was perpendicular to the DG grooves (s polarisation [5]). The laser frequency was tuned from one spectral line to another by rotating the DG. The laser cavity contained an aperture placed near the DG, whose diameter was varied from 10 to 30 mm in different experiments. The laser emission spectrum was detected with a slit spectrograph with a 2.5-m focal length. The laser emission was visualised by an IR video camera. To identify the spectral lines of overtone emission, we calculated the wavelengths of spectral lines corresponding to the overtone vibrational-rotational transitions of the CO molecule.

We used in the experiments three reflecting DGs (DG1 – DG3), which were blazed for nonpolarized light at 3.0 μm (DG1, 200 lines mm^{-1}), 2.15 μm (DG2, 420 lines mm^{-1}), and 3.2 μm (DG3, 200 lines mm^{-1}). The DGs were made of glass with aluminium (DG1 and DG3) and gold (DG2) coatings. To measure the reflection (outcoupling) coefficient T for the radiation outcoupled into the zero order of the grating operating in the autocollimation scheme (see Figs 1c, 2b, and 3c), we placed a plane-parallel CaF_2 plate into the laser cavity. It was positioned between the Brewster window and the DG. The coefficient T was defined as the ratio of energies of the radiation outcoupled into the zero order and the radiation reflected from the plate.

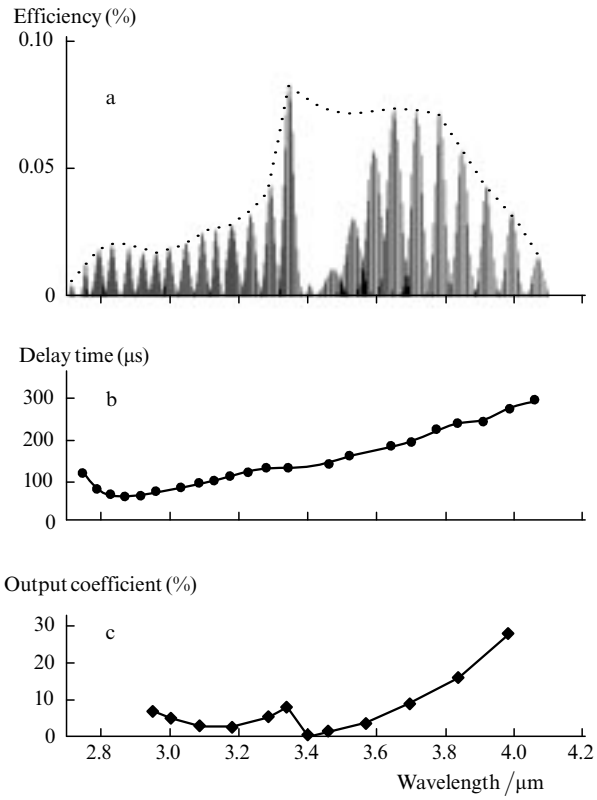

Figure 1. Dependences of (a) the output laser efficiency, (b) the time delay of a laser pulse onset, and (c) the outcoupling coefficient T for the zero order of the DG1 on the wavelength for the CO : He = 1 : 4 mixture and the specific input energy 320 J l^{-1} amagat^{-1}.

3. Output laser characteristics

3.1. Spectral and energy characteristics

The widest spectral tuning range in the overtone CO laser was observed for the frequency-selective cavity with the DG1. Fig. 1 presents some characteristics of this laser for the spectral lines corresponding to overtone vibrational-rotational lines of the CO molecule. In this case, we obtained tuning in the 2.71 – 4.09-μm range, which corresponded to vibrational transitions from $12 \rightarrow 10$ to $37 \rightarrow 35$. In the short-wavelength region below 2.7 μm, the emission spectrum was limited by the intracavity absorption of radiation by water vapour. In the long-wavelength region above 4.0 μm, it was limited by the cavity Q-factor, because the outcoupling coefficient increased nearly to 30 %.

The laser with the DG1 had a well-pronounced dip in the wavelength dependence of the laser efficiency at 3.4 μm. The maximum laser efficiency decreased from ~ 0.1 % at the centre of the $26 \rightarrow 24$ vibrational band to nearly zero at the centre of the neighbouring $27 \rightarrow 25$ band. Unlike the laser efficiency, the delay time of the onset of the laser pulse relative to the pump pulse had a monotonic behaviour in this spectral region (Fig. 1b). The nonuniformity of spectral and energy characteristics of the overtone CO laser in this spectral region was caused by a sharp decrease (down to 0.5 %) in the coefficient T for the radiation outcoupled into the zero diffraction order [5] (Fig. 1c).

The maximum laser efficiency in the frequency-selective regime (~ 0.1 %) was obtained in the spectral ranges where T (Fig. 1c) was 5 – 10 % (for instance, in the 3.6 – 3.8 μm range). The laser efficiency in the 3.4 – 3.6-μm range, which corresponded to the dip in Fig. 1a, was increased by using an additional intracavity CaF_2 plate for increasing the outcoupling coefficient (the dashed curve in Fig. 1a represents the envelope of efficiency peaks in each vibrational band).

The efficiency of the frequency-selective overtone CO laser with the DG2 and the outcoupling coefficient T for this grating as functions of the wavelength is shown in Fig. 2. In these experiments, we used the CO : N_2 = 1 : 9 mixture at 100 K with a density of 0.12 amagat. The specific input energy was 360 J l^{-1} amagat^{-1}. Lasing was observed in the spectral range from 2.84 to 4.02 μm, which corresponds to the vibrational transitions from $15 \rightarrow 13$ to $36 \rightarrow 34$. Using a nitrogen-containing mixture, we managed to increase considerably the specific output energy and the efficiency of the overtone CO laser. In these experiments, their maximum values (1.3 J l^{-1} amagat^{-1} and 0.34 %, respectively) were obtained for the $34 \rightarrow 32$ $P(12)$ and $P(13)$ vibrational-rotational transitions at $\lambda \approx 3.83$ μm.

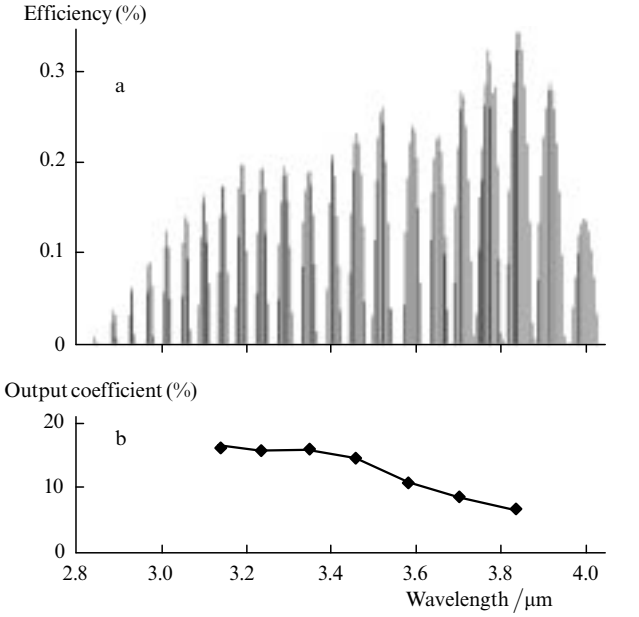

Figure 2. Dependences of (a) the output laser efficiency and (b) the outcoupling coefficient T for the zero order of the DG2 on the wavelength for the CO : N_2 = 1 : 9 mixture and the specific input energy 360 J l^{-1} amagat^{-1}.

The laser with the DG3 and the CO : He = 1 : 4 mixture (Fig. 3a) had a tuning range of 3.27 – 4.17 μm, with the maximum efficiency near 3.71 μm (the specific input energy was 320 J l^{-1} amagat^{-1}). The spectral range was limited in the short-wavelength region because of the non-optimum outcoupling of radiation into the zero order (Fig. 3c). The spectral characteristic of the laser cavity in the long-wavelength region (~ 4.0 μm) was closer to the optimum one, because the outcoupling coefficient was ~ 8 % in contrast to 30 % for the laser with the DG1. Under these experimental conditions, we have observed for the first time lasing on the $38 \rightarrow 36$ vibrational transition. In the case of the CO : N_2 = 1 : 6 mixture and the DG3, the efficiency of the frequency-selective overtone CO laser for the $34 \rightarrow 32$ transition at the wavelength ~ 3.84 μm was increased up to 0.55 % (Fig. 3b), but lasing on the $38 \rightarrow 36$ transition was absent. Fig. 4 presents the vibrational-rotational struc-

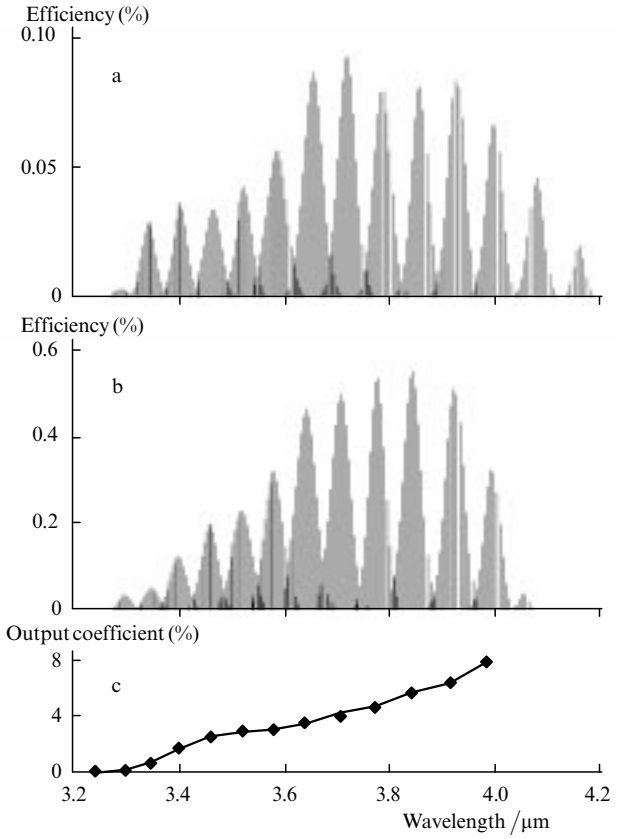

Figure 3. Dependences of (a, b) the output laser efficiency and (c) the outcoupling coefficient T for the zero order of the DG3 on the wavelength for the (a) CO : He = 1 : 4 and (b) CO : N_2 = 1 : 6 gas mixtures and the specific input energies (a) 320 and (b) 500 J l^{-1} amagat^{-1}.

ness of the resonance between the 0 → 1 vibrational transition of the N_2 molecule and the 40 → 38 overtone vibrational transition of the CO molecule (vibrational-vibrational change of two vibrational quanta for a single one).

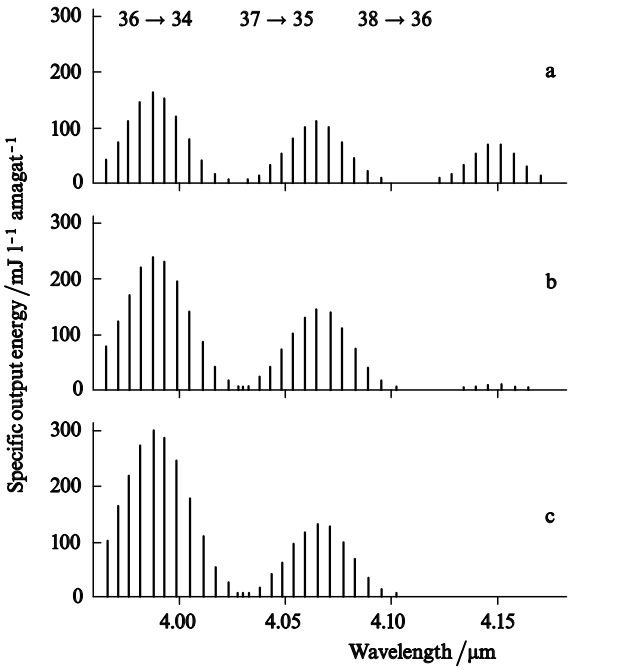

Figure 4. Spectral dependences of the specific output energy of the laser with the DG3 emitting in the range corresponding to three vibrational bands 36 → 34, 37 → 35, and 38 → 36 for nitrogen concentrations of (a) 0, (b) 3.3, and (c) 10% in the CO : He = 1 : 4 mixture.

ture of the emission spectrum of the overtone CO laser for the 36 → 34, 37 → 35, and 38 → 36 vibrational transitions for different nitrogen concentrations in a gas mixture. An increase in the content of nitrogen in the CO : He = 1 : 4 mixture caused an increase in the specific output energy emitted in the 36 → 34 vibrational transition and a decrease in the specific output energy in the 38 → 36 transition. The experiments showed that no lasing was observed on the 38 → 36 transition when ~ 10% of nitrogen was added into the CO : He mixture. It is likely that this is caused by the close-

A complete list of 430 vibrational-rotational transitions that produced overtone laser emission in the experiments, both in frequency-selective and in multifrequency regimes (see also [1]), is presented in the Table 1.

Within the limits of one vibrational-rotational band, the overtone CO laser emission was tuned over several (sometimes more than 20) vibrational-rotational lines. Fig. 5 shows the dependence of the specific output energy on the rotational quantum number J of the component in the 32 → 30 vibrational band for specific input energies of

Table 1. Overtone vibrational-rotational transitions of the CO molecule on which lasing was observed (430 lines).

$v+2 \rightarrow v$	$P(J)$	$v+2 \rightarrow v$	$P(J)$	$v+2 \rightarrow v$	$P(J)$
6 → 4*	$P(11)-P(13)$	17 → 15	$P(8)-P(20)$	28 → 26	$P(4)-P(23)$
7 → 5*	$P(11)-P(13)$	18 → 16	$P(7)-P(18)$	29 → 27	$P(4)-P(24)$
8 → 6*	$P(11)-P(13)$	19 → 17	$P(6)-P(17)$	30 → 28	$P(4)-P(24)$
9 → 7*	$P(11)-P(13)$	20 → 18	$P(6)-P(18)$	31 → 29	$P(4)-P(24)$
10 → 8*	$P(11)-P(13)$	21 → 19	$P(6)-P(18)$	32 → 30	$P(4)-P(24)$
11 → 9*	$P(11)-P(13)$	22 → 20	$P(5)-P(16)$	33 → 31	$P(4)-P(23)$
12 → 10	$P(11)-P(15)$	23 → 21	$P(4)-P(18)$	34 → 32	$P(4)-P(23)$
13 → 11	$P(10)-P(16)$	24 → 22	$P(4)-P(17)$	35 → 33	$P(4)-P(24)$
14 → 12	$P(7)-P(19)$	25 → 23	$P(4)-P(21)$	36 → 34	$P(4)-P(21)$
15 → 13	$P(7)-P(19)$	26 → 24	$P(4)-P(21)$	37 → 35	$P(6)-P(19)$
16 → 14	$P(9)-P(19)$	27 → 25	$P(4)-P(22)$	38 → 36	$P(10)-P(17)$

*Transitions on which lasing was observed in multifrequency regime[1].

200, 400, and 550 J l^{-1} amagat^{-1} in the laser with the DG1 and the CO : N_2 = 1 : 9 mixture. As the specific input energy was increased, the maximum efficiency of the laser, which was tuned over rotational lines within one vibrational band, shifted to greater numbers J from $J = 11$ at a specific input energy of 200 J l^{-1} amagat^{-1} (Fig. 5a) to $J = 15$ at 550 J l^{-1} amagat^{-1} (Fig. 5c). The shift of the efficiency maximum was caused by an increase in the translational and rotational temperatures of gas molecules with increasing pump pulse energy.

The spectral range in which we observed lasing on high-lying transitions in the overtone CO laser is of interest because it lies in the atmospheric transparency window. Because of this, we experimentally studied the effect of the density of a gas laser medium and its composition on the energy characteristics of laser emission in the region of high-lying transitions.

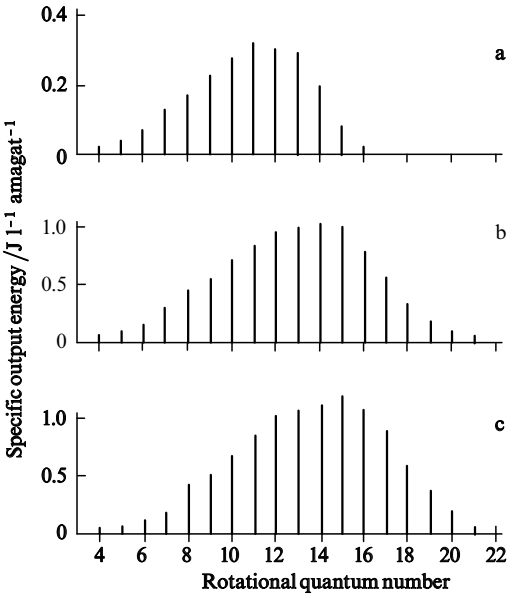

Figure 5. Dependences of the specific output energy of the laser with the DG1 on the rotational quantum number J of the rotational component of the 32 → 30 vibrational band for the specific input powers (a) 200, (b) 400, and (c) 550 J l^{-1} amagat^{-1} and the CO : N_2 = 1 : 9 mixture.

The dependences of the specific output energy of the laser with the DG1 on the specific input energy for three vibrational-rotational lines $P(9)$, $P(13)$, and $P(16)$ of the 36 → 34 vibrational band for different densities N of the CO : N_2 = 1 : 9 mixture are presented in Fig. 6. Note that the threshold specific input energy increased with increasing number J, the gas density being fixed. As the density of a gas medium was increased, the threshold specific input energy at which the specific output energy reached a maximum decreased. For the spectral line with the largest J [in our experiments, for the $P(16)$ line], the maximum specific output energy increased from ~ 50 mJ l^{-1} amagat^{-1} at $N = 0.05$ amagat to ~ 200 mJ l^{-1} amagat^{-1} at $N = 0.3$ amagat. For the $P(13)$ line, the effect of the gas density on the specific output energy was weaker. As for the $P(9)$ line, an increase in N from 0.09 to 0.3 amagat even caused a decrease in the specific output energy.

Fig. 7 shows the efficiency of the laser with the DG1 operating on the 35 → 33 $P(12)$ line as a function of the specific input energy for five different gas mixtures. For different gas mixtures, the efficiency reached a maximum at different specific input energies from ~ 250 J l^{-1} amagat^{-1} for the CO : He = 1 : 4 mixture to ~ 650 J l^{-1} amagat^{-1} for the CO : N_2 = 1 : 1 mixture. In this experiment, the highest laser efficiency (~ 0.18 %) was obtained for the CO : N_2 = 1 : 9 mixture (at a specific input energy of ~ 400 J l^{-1} amagat^{-1}). A decrease in laser efficiency with increasing specific input energy above the optimum value is caused by the gas mixture superheating.

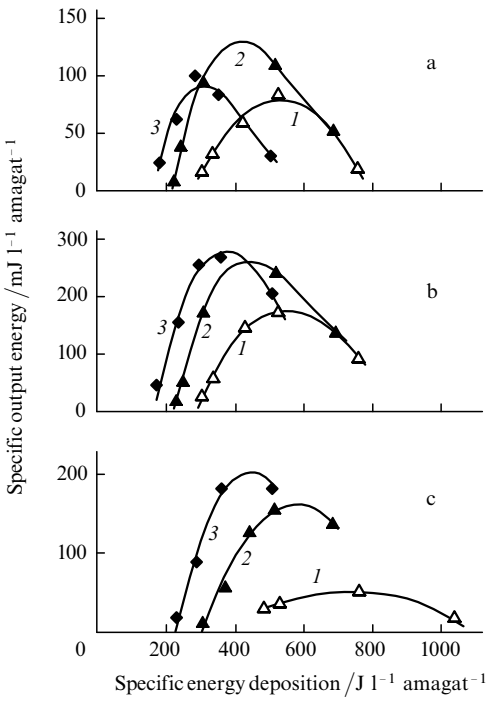

Figure 6. Dependences of the specific output energy of the laser with the DG1 emitting at three spectral lines (a) $P(9)$, (b) $P(13)$, and (c) $P(16)$ of the 36 → 34 vibrational transition on the specific input energy for the CO : N_2 = 1 : 9 mixture with a density of (1) 0.05, (2) 0.09, and (3) 0.3 amagat.

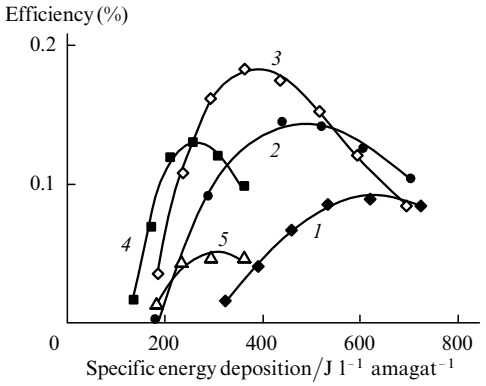

Figure 7. Dependences of the output efficiency of the laser with the DG1 emitting at the 35 → 33 $P(12)$ line on the specific input energy for (*1*) CO : N_2 = 1 : 1, (*2*) CO : N_2 = 1 : 4, (*3*) CO : N_2 = 1 : 9, (*4*) CO : N_2 : : He = 1 : 9 : 10, and (*5*) CO : He = 1 : 4 mixtures.

3.2. Small-signal gain

Lasing in the 36 → 34 band at ~ 4.0 μm was observed even in the case of a low Q factor of the cavity with the DG1 (Fig. 1a). In this case, the outcoupling coefficient T reached

30 % (Fig. 1c), and the total round-trip loss of radiation in the laser cavity weres as high as 35 – 40 %. In the laser cavity with this optical loss, lasing is excited when the small-signal gain exceeds 0.2 m^{-1}.

In Refs [6 – 8], the maximum small-signal gain in the active medium of a multifrequency overtone electroionisation CO laser with an intracavity spectral filter was measured using the calibrated optical loss technique. The gain was found to be ~ 0.15 m^{-1}, but the laser radiation wavelength was not greater than 3.6 μm. Using the same technique, we made experiments with the laser having a frequency-selective cavity, the DG1, and additional intracavity loss of up to 35 %. We observed lasing in the CO : N_2 = 1 : 9 mixture on the 34 → 32 $P(12)$ line at 3.84 μm for the total round-trip loss of up to ~ 55 %, and the threshold specific input energy under these conditions was ~ 250 J l^{-1}amagat^{-1}. The results of this experiment allow us to estimate the small-signal gain in the active medium of the overtone CO laser for this spectral line as 0.35 m^{-1}.

3.3. Time characteristics of laser emission

Fig. 8 presents the time delay τ of the onset of a laser pulse relative to the onset of a pump pulse as a function of the rotational quantum number J of a component in the 32 → 30 vibrational band for different specific input energies. The results correspond to the laser with the DG1. The time delay for different rotational lines was nearly the same, and its value slowly increased towards the wings of the vibrational band. As the specific input energy was increased, the time delay decreased, and its minimum value for each curve, which differed from the maximum value by 10 – 15 %, shifted in the direction of increasing rotational quantum number. A decrease in the density of a gas medium caused a substantial increase in τ and the pulse length. For the 36 → 35 $P(13)$ line, the time delay τ and the pulse length increased from ~ 120 μs and 0.6 ms at a gas density of 0.3 amagat to ~ 900 μs and 2.2 ms at 0.05 amagat, other experimental conditions being the same (a specific input power of 300 J l^{-1} amagat^{-1}, CO : N_2 = 1 : 9 mixture).

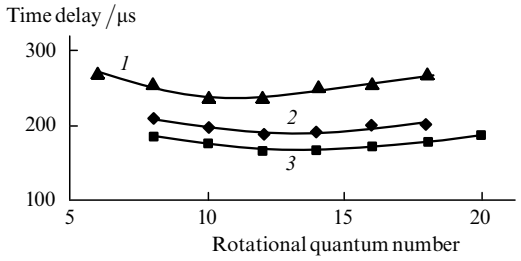

Figure 8. Delay times of the onset of a laser pulse versus the rotational quantum number J of the rotational component of the 32 → 30 vibrational band for the specific input energy (*1*) 300, (*2*) 400, and (*3*) 550 J l^{-1} amagat^{-1} for the DG1 and the CO : N_2 = 1 : 9 mixture.

Fig. 1b shows the dependence of the delay time τ on the laser wavelength within the tuning range from the 12 → 10 vibrational band to the 37 → 35 band. The time delay τ varied from ~ 60 to ~ 350 μs. In the 3.4-μm region, the outcoupling coefficient deceased down to 0.5 % (Fig. 1c). However, unlike the laser efficiency (Fig. 1a), the delay time τ of the onset of a pulse of overtone laser emission had a monotonic behaviour in this spectral region (Fig. 1b), i. e., an increase in the cavity Q factor had almost no effect on τ. The results of this experiment suggest that the time delay of the onset of laser emission on spectral lines of the overtone CO laser is predominantly determined by the inversion formation time for overtone transitions of the CO molecule rather than by the achievement of the threshold small-signal gain.

3.4. Calculation results, their analysis, and comparison with the experiment

The characteristics of the frequency-selective CO laser operating on the first vibrational overtone were studied using two theoretical models of vibrational kinetics. We used the model taking into account the multiquantum VV exchange (MQE) [9], which is most realistic nowadays, and the conventional model based on the single-quantum VV exchange (SQE) [7]. To determine more exactly the applicability of these two models to the study of characteristics of the overtone CO laser, their results were compared with one another and the experimental data. Laser characteristics were simulated for two mixtures (CO : N_2 = 1 : 9 and 1 : 6) that gave the best energy characteristics in the experiments using the DG2 and DG3 (Figs 2a and 3b).

In the calculations, we used the same parameters of the active medium, the pump, and the laser energy as in the experiment. The specific input energy was chosen in a range

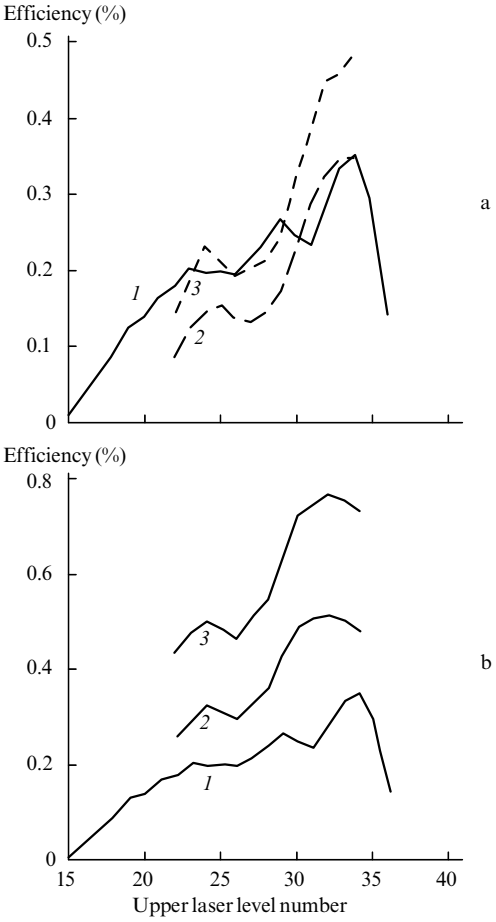

Figure 9. (*1*) Experimental and (*2*, *3*) calculated dependences of the output laser efficiency on the the number of the upper laser level $v + 2$ for the CO : N_2 = 1 : 9 mixture and the specific input energy 360 Jl^{-1}amagat^{-1}. The calculations using (a) multiquantum and (b) single-quantum models were made for round-trip loss of (2) 7.5 and (3) 5.5% introduced into the cavity by the DG2.

of 200 – 650 J l^{-1} amagat^{-1}, the initial temperature was 100 K, and the gas density was $N = 0.12$ amagat. The fraction of radiation outcoupled from the cavity was specified in accordance with the experimentally determined reflection coefficients of DGs (see Figs 2b and 3c). In the absence of exact data on the cavity loss through absorption and scattering of radiation by DG2 and DG3, this additional loss was used as a wavelength-independent parameter. The corresponding tuning curves (the dependences of the selective-lasing efficiency on the number of the upper laser level $v+2$ for the $v+2 \rightarrow v$ transition) calculated for the $CO : N_2 = 1 : 9$ mixture and additional round-trip loss of 7.5 and 5.5 % within the framework of the MQE model are compared in Fig. 9a with the experimental results. One can clearly see that the best agreement with the experiment is obtained under the assumption that the additional loss increases with increasing number of the vibrational transition being selected.

The results obtained for the same conditions using the SQE model (see Fig. 9b) are characterised by the same form of tuning curves, but considerably overstate the output laser efficiency. The results of simulation for the $CO : N_2 = 1 : 6$ mixture were more sensitive to the choice of the kinetic model. In Fig. 10, the results of these two models for the given mixture are compared with the experimental results obtained for an additional round-trip loss of 6.8 %.

One can see that the MQE model provides a good agreement with the experiment, both in the form of the tuning curve and in its amplitude, which is not provided by the SQE model. To estimate the limiting achievable efficiency of the overtone selective lasing, we made additional calculations using the MQE model. For the $CO : N_2 = 1 : 6$ mixture under the conditions of Fig. 10, the calculations gave for the $29 \rightarrow 27$ ($J = 15$) transition an efficiency of ~ 1 %, with additional round-trip loss being equal to 3 %.

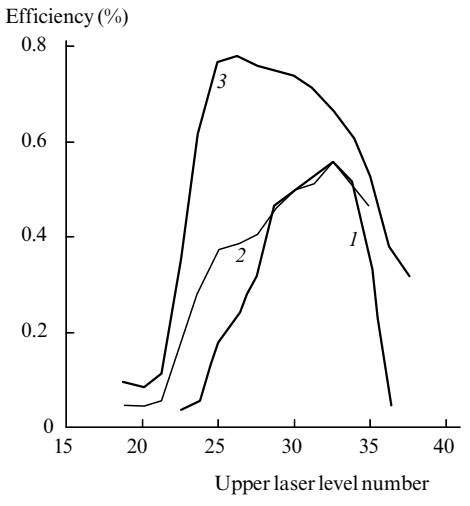

Figure 10. Experimental dependences of the output laser efficiency on the number $v+2$ (*1*) and the dependences calculated using MQE (*2*) and SQE (*3*) models for the experimental conditions corresponding to Fig. 3b.

Using the MQE model, we also calculated the laser energy emitted in the $32 \rightarrow 30$ band as a function of the number of the rotational component of the *P*-branch. The calculations were made for the conditions corresponding to the experimental spectra in Fig. 5. The calculated spectra, which are presented in Fig. 11, agree with the experiment. Note that the agreement of the results of the conventional SQE model with the experiment was considerably worse. This fact is illustrated by the comparison of the spectrum calculated in the SQE approximation (Fig. 12a), the experimental spectrum (Fig. 12c), and the spectrum calculated using the MQE model (Fig. 12b). The use of the SQE model causes a considerable depletion of the spectrum on the side of small J and its narrowing as a whole.

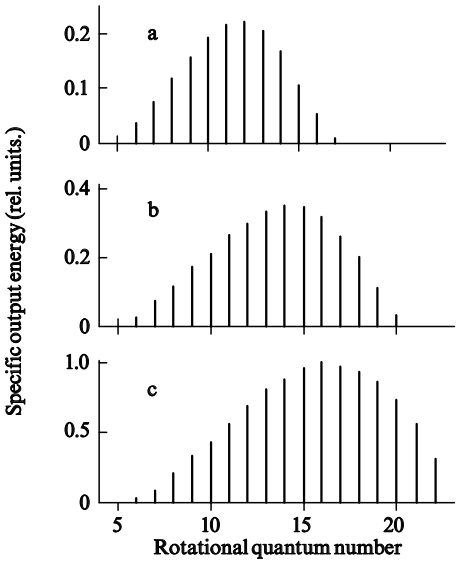

Figure 11. Calculated dependences of the specific output energy of the laser with the DG1 on the rotational quantum number J of a component in the $32 \rightarrow 30$ vibrational band for the specific input energy 200 (a), 400 (b), and 550 J l^{-1} amagat^{-1} (c) and the $CO : N_2 = 1 : 9$ mixture.

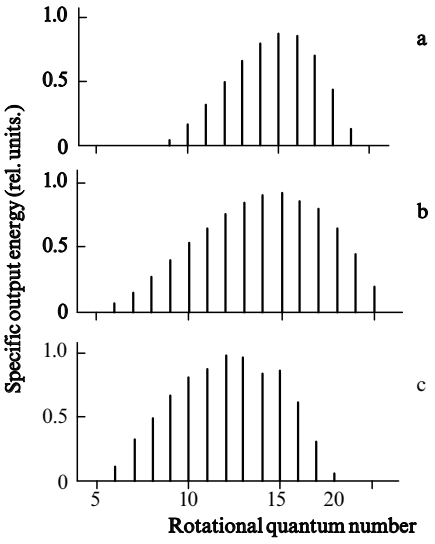

Figure 12. Dependences of the specific output energy of the laser with the DG1 on the rotational quantum number J of a component in the $32 \rightarrow 30$ vibrational band calculated using (a) SQE and (b) MQE models and (c) experimentally measured for the $CO : N_2 = 1 : 9$ mixture and the specific input energy 360 J l^{-1} amagat^{-1}.

The dependences presented in Fig. 8 for the time delay of the beginning of a laser pulse as a function of the number of the rotational component of the P branch being selected in

the $32 \rightarrow 30$ band can be used to estimate the ratio of vibrational populations of the lower and upper laser levels N_v/N_{v+2} at the moment when the threshold for the marginal transitions is reached. According to the Patel formula, the gain for separate rotational components of the P branch in the $v+2 \rightarrow v$ band has the form

$$g_{v,J} \sim \alpha(J) = \sigma_{v,J}(1 - \delta_{v,J}N_v/N_{v+2}), \quad (1)$$

where $\sigma_{v,J}$ is the cross section for induced transitions at the central frequency and $\delta_{v,J}$ is the factor expressed in terms of the ratio of statistical weights and populations of rotational levels. The gain coefficient $g_{v,J}$ depends on the ratio of populations N_v/N_{v+2} and the translational temperature T_0 (because of $\sigma_{v,J}$ and $\delta_{v,J}$), which enables one to estimate N_v/N_{v+2} at the given T_0. The corresponding dependences $\alpha(J)$, constructed using formula (1) for different values of N_{30}/N_{32}, are presented in Fig. 13. They illustrate a high sensitivity of gain to the value of N_{30}/N_{32}. This sensitivity justifies the implicit assumption that the dependence of gain on J and time is determined only by a change in the bracketed expression in (1). The temperature T_0 was taken from the numerical calculation made for the conditions of Fig. 8 (curve *2*).

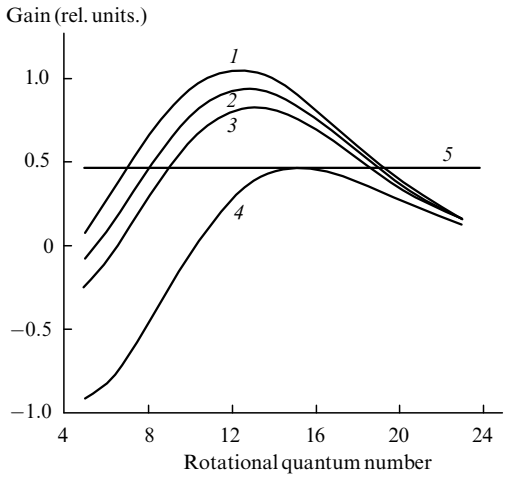

Figure 13. Dependences $\alpha(J)$ for the $32 \rightarrow 30$ vibrational band and $N_{30}/N_{32} =$ (*1*) 1.07, (*2*) 1.095, (*3*) 1.12, and (*4*) 1.222; curve 5 corresponds to the threshold gain. The calculations were made for the same conditions as in Fig. 8 (curve *2*).

Curve *2* in Fig. 13, which was plotted for $N_{30}/N_{32} = 1.095$, corresponds to the equality $\tau(J = 8) \approx \tau(J = 19)$ observed in the experiment (Fig. 8, curve *2*). Assuming that the equality $\alpha(8) = \alpha(19)$ at $N_{30}/N_{32} = 1.095$ corresponds to the threshold gain (Fig. 13, curve *5*), we shall estimate the ratio N_{30}/N_{32} at which the laser threshold for the transition with $J = 14$ is achieved earlier than the thresholds for all other lasing transitions that were observed in the experiment [the difference of time delays for the transitions with $J = 14$ and $J = 8$ ($J = 19$) is 25 μs]. Curve *4* in Fig. 13 reaches the threshold value at $N_{30}/N_{32} = 1.222$. Thus, one can find from the experimental dependence $\tau(J)$ (see Fig. 8), using no complicated kinetic model, that the ratio of populations of the levels 30 and 32 changed in 25 μs from 1.222 to 1.095. The comparison of this statement with the numerical calculation gives one more argument in favour of the applicability of the MQE model. The reliability of such estimates depends on the accuracy of determination of T_0. When T_0 is changed by +10 K and −10 K from the value corresponding to the dependences in Fig. 13, the ratios N_{30}/N_{32} providing the validity of the condition $\alpha(8) \approx \alpha(19)$ become equal to 1.086 and 1.12, i. e., change by no more than 2.5 %.

The dependence of the time delay on the number of the rotational transition in a fixed vibrational band, calculated using the MQE model, agrees well with the experiment. Fig. 14 compares the calculated and the experimentally observed 'relative' time delays $\Delta\tau$ for the $32 \rightarrow 30$ band for different specific input energies, i. e., the time delays calculated from the minimum values of τ. One can see that the experimental and calculated dependences $\Delta\tau(J)$ are in a good agreement, which supports the adequacy of our simulation of the vibrational kinetics.

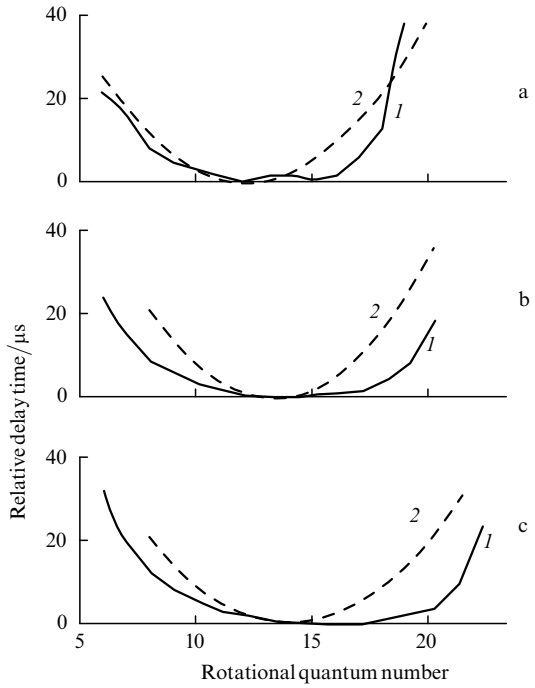

Figure 14. (*1*) Theoretical and (*2*) experimental dependences of the relative time delay of a laser pulse on the rotational quantum number of a component in the $32 \rightarrow 30$ vibrational band for the specific input energy (a) 300, (b) 400, and (c) 550 J l^{-1} amagat^{-1}.

In our opinion, the energy efficiency of lasing on a separate line is unlikely to be substantially higher than 1 %. One can obtain a higher efficiency for the given transition in a narrow-band cavity that selects frequencies of 3 – 5 neighbouring vibrational transitions [1, 10]. Under these conditions, a considerable concentration of energy on the lowest one of these transitions in the radiative cascade is obtained.

4. Conclusions

We have studied experimentally and theoretically frequency-selective lasing in the pulsed electroionisation CO laser operating on the first overtone of the CO molecule. The small-signal gain in the experiments exceeded 0.35 m^{-1}. The specific output energy and the electrooptical efficiency of the overtone CO laser in the frequency-selective regime reached ~ 3 J l^{-1} amagat^{-1} and ~ 0.6 %. Lasing was observed on 413 vibrational-rotational transitions. We have observed for

the first time lasing on the high-lying $38 \rightarrow 36$ vibrational transition and observed the influence of nitrogen additions into a laser mixture on its efficiency.

Our study shows that the pulsed overtone electroionisation CO laser is an efficient source of tunable coherent emission in the 2.7 – 4.2-μm range. The emission spectrum of the pulsed overtone laser, including the vibrational-rotational transitions, lies in the 2.5 – 4.2-μm range and overlaps the spectral range of HF and DF lasers. Note that the density of vibrational-rotational lines in this range is higher than that for the latter two lasers.

The comparison of experimental and theoretical data showed their agreement for spectral and energy characteristics of emission of the overtone CO laser and revealed the necessity of taking into account the MQE processes on high-lying vibrational levels [8, 9]. The use of the MQE model provided a better agreement with the experiment in the output efficiency of lasing on a separate vibrational-rotational transition in a wide range of vibrational and rotational quantum numbers and describes adequately the relative time delay of lasing on separate rotational components in a fixed vibrational band. The theoretical analysis shows that the efficiency of the overtone CO laser with intracavity selection of vibrational-rotational lines may reach 1 %.

Acknowledgements. The authors thank H Ackerman of AFRL, J McIver of the University of New Mexico, and M. Stickley of EOARD for their help in organising this joint study. This work was supported by the Russian Foundation for Basic Research, Grant No. 99-02-17553.

References

1. Basov N G, Ionin A A, Kotkov A A, Kurnosov A K, et al. *Kvantovaya Electron. (Moscow)* **30** 771 (2000) [*Quantum Electron.* **30** 771 (2000)]
2. Gromoll-Bohle M, Bohle W, Urban W *Opt. Commun.* **69** 409 (1989)
3. Bachem E, Dax A, Fink T, Weidenfeller A, et al. *Appl. Phys. B* **57** 185 (1993)
4. Murtz M, Frech B, Palm P, Lotze R, Urban W *Opt. Lett.* **23** 58 (1998)
5. Palmer C (Ed.) *Diffraction Grating Handbook, 3rd ed.* (New York: Richardson Grating Laboratory, 1996)
6. Ionin A, Kotkov A, Kurnosov A, Napartovich A, et al. *Proc. Int. Conf. LASERS'97, New Orleans, LA, USA, 1977* (STS Press, McLean, VA, 1998) p. 92
7. Ionin A A, Klimachev Yu M, Kotkov A A, Kurnosov A K, et al. Preprint No. 11/1998 (Moscow: P N Physics Institute, 1998)
8. Ionin A, Kotkov A, Kurnosov A, Napartovich A, et al. *Opt. Commun.* **155** 197 (1998)
9. Ionin A A, Klimachev Yu M, Kotkov A A, Kurnosov A K, et al. Preprint No. 70/1999 (Moscow: P N Lebedev Physics Institute, 1999)
10. Ionin A A, Kotkov A A, Kurnosov A K, Napartovich A P, et al. *Opt. Commun.* **160** 225 (1999)